



20th European Conference on Fracture (ECF20)

An experimental compliance calibration strategy for mixed-mode bending tests

Stefano Bennati^{a,*}, Paolo S. Valvo^a

^a University of Pisa, Department of Civil and Industrial Engineering, Largo Lucio Lazzarino, I 56122 Pisa (PI), Italy

Abstract

We have developed an enhanced beam theory model of the mixed-mode bending (MMB) test, where the delaminated specimen is schematised as an assemblage of sublaminates connected by an elastic interface. We show how the interface parameters can be estimated through an experimental compliance calibration strategy. First, double cantilever beam (DCB) and end notched flexure (ENF) tests are conducted and the specimens' compliance is measured. Then, a nonlinear least squares fitting procedure furnishes the values of the elastic interface constants. Such calibrated values can be used to interpret the results of MMB tests.

© 2014 Published by Elsevier Ltd. This is an open access article under the CC BY-NC-ND license

(<http://creativecommons.org/licenses/by-nc-nd/3.0/>).

Selection and peer-review under responsibility of the Norwegian University of Science and Technology (NTNU), Department of Structural Engineering

Keywords: mixed-mode fracture; energy release rate; virtual crack closure technique

1. Introduction

The mixed-mode bending (MMB) test is used to determine the delamination toughness of fibre-reinforced composite laminates under I/II mixed mode fracture conditions (ASTM 2006). The MMB test can be regarded as the superposition of the double cantilever beam (DCB) and end notched flexure (ENF) tests, respectively used for pure fracture modes I and II (Adams et al. 2003, AECMA 1995a, 1995b).

We have developed an enhanced beam-theory (EBT) model of the MMB test, wherein the delaminated specimen is schematised an assemblage of two identical sublaminates partly connected by a deformable interface. The

* Corresponding author. Tel.: +39-050-2218200; fax: +39-050-2218201.

E-mail address: s.bennati@ing.unipi.it

sublaminates are modelled as extensible, flexible, and shear-deformable laminated beams. The interface is regarded as a continuous distribution of linearly elastic–brittle springs. An exact analytical solution for the internal forces, displacements, and interfacial stresses has been deduced (Bennati et al. 2013a) and approximate expressions for the specimen's compliance, energy release rate, and mode mixity have been determined (Bennati et al. 2013b).

The predictive effectiveness of the aforementioned model relies on the accurate estimation of the values of the elastic interface constants. Here, we show how the values of such parameters can be estimated through an experimental compliance calibration strategy. To this aim, DCB and ENF tests are conducted on the considered type of specimen and experimental measures of compliance are determined. Then, a nonlinear least squares fitting procedure is applied to deduce the values of the elastic interface constants. Lastly, such calibrated values can be used to interpret the results of MMB tests.

2. The mixed-mode bending test

2.1. Mechanical model

In the MMB test, a laminated specimen endowed with a pre-implanted delamination of length a (Fig. 1b) is simply supported and loaded through a rigid lever (Fig. 1a). We denote with L , B , and H the specimen's length, width, and thickness, respectively. The delamination divides the specimen into two sublaminates, each of thickness $h = H/2$. The load applied by the testing machine, P , is transferred to the specimen as an upward load, P_u , and a downward load, P_d . The lever arm lengths, c and d , can be adjusted to vary the intensities of P_u and P_d and, consequently, impose a desired I/II mixed-mode ratio, $\alpha = G_I/G_{II}$. For what follows, it is useful to define the lengths $b = L - a$ and $\ell = L - d$. According to ASTM (2006), the downward load, P_d , is applied at the specimen's mid-span section, so that $\ell = d = L/2$. Global reference x - and z -axes are fixed, aligned with the specimen's longitudinal and transverse directions, respectively.

According to the enhanced beam-theory (EBT) model, the sublaminates may have any stacking sequences, provided that they behave as plane beams and have no shear-extension or bending-extension coupling (Bennati et al. 2013a). In line with classical laminated plate theory (Jones 1999), we denote with A_1 , C_1 , and D_1 the sublaminates' extensional stiffness, shear stiffness, and bending stiffness, respectively. For orthotropic specimens, $A_1 = E_x h$, $C_1 = 5 G_{xz} h/6$, and $D_1 = E_x h^3/12$, where E_x and G_{xz} are the longitudinal Young's modulus and transverse shear modulus. The sublaminates are partly connected by a deformable interface, regarded as a continuous distribution of linearly elastic–brittle springs. We denote with k_z and k_x the elastic constants of the distributed springs respectively acting along the normal and tangential directions with respect to the interface plane (Fig. 1c).

2.2. Specimen's compliance

For a linearly elastic load-deflection response, the specimen's compliance is defined as $C = \delta/P$, where P is the applied load and δ is the displacement of the load application point (Adams et al. 2003). According to the EBT model, the MMB test specimen's compliance turns out to be

$$C_{\text{MMB}} = \left(\frac{3c - \ell}{4\ell}\right)^2 C_{\text{DCB}} + \left(\frac{c + \ell}{\ell}\right)^2 C_{\text{ENF}}, \quad (1)$$

where

$$C_{\text{DCB}} = \frac{2a^3}{3BD_1} + \frac{2a}{BC_1} + \frac{2}{\lambda_1 \lambda_2 B D_1} \left[(\lambda_1 + \lambda_2) a^2 + 2a + \frac{1}{\lambda_1} + \frac{1}{\lambda_2} \right] \quad \text{and} \quad (2)$$

$$C_{\text{ENF}} = \frac{1}{24B} \frac{A_1 h^2}{A_1 h^2 + 4D_1} \left(\frac{a^3}{D_1} + \frac{8\ell^3}{A_1 h^2} \right) + \frac{\ell}{4BC_1} + \frac{1}{8BD_1} \frac{A_1 h^2}{A_1 h^2 + 4D_1} \frac{1}{\lambda_5^2} \left[\lambda_5 a^2 + a + 2\ell - \frac{2}{\lambda_5} - \frac{4a}{\exp \lambda_5 (\ell - a)} \right]$$

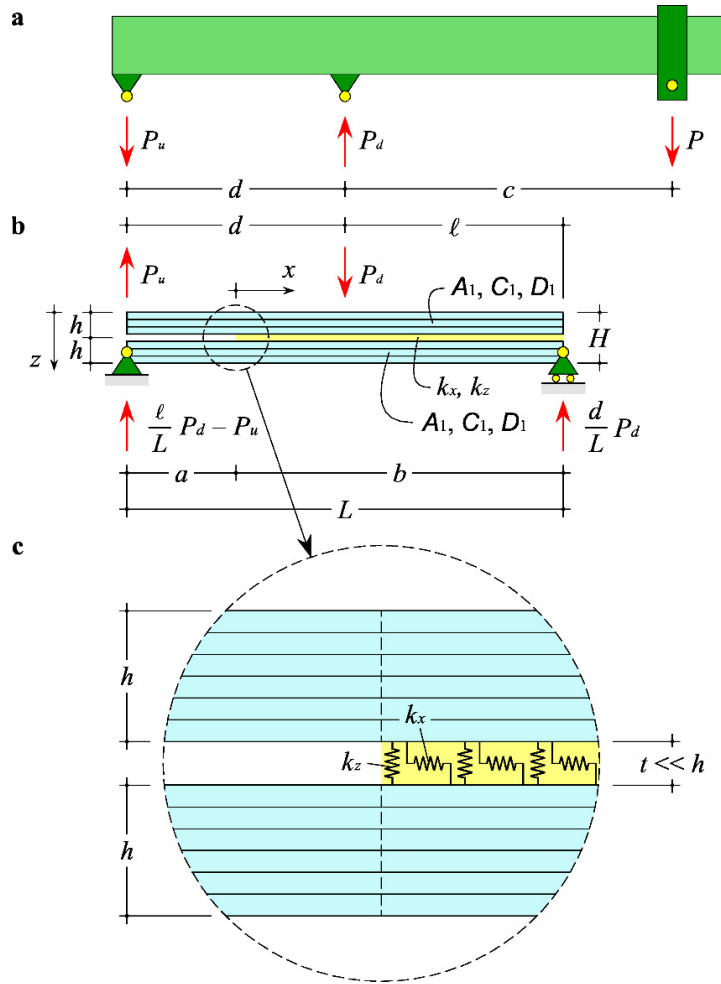


Fig. 1. MMB test: (a) loading lever; (b) laminated specimen; (c) detail of the crack tip region and elastic interface.

are the compliances of the DCB and ENF test specimens, respectively. In Eqs. (2),

$$\lambda_1 = \sqrt{\frac{k_z}{C_1} \left(1 + \sqrt{1 - \frac{2 C_1^2}{k_z D_1}}\right)}, \quad \lambda_2 = \sqrt{\frac{k_z}{C_1} \left(1 - \sqrt{1 - \frac{2 C_1^2}{k_z D_1}}\right)}, \quad \text{and} \quad \lambda_3 = \sqrt{2 k_x \left(\frac{1}{A_1} + \frac{h^2}{4 D_1}\right)} \quad (3)$$

are the roots of the characteristic equations of the governing differential problem (Bennati et al. 2013a).

Interestingly, Eqs. (2) show that C_{DCB} and C_{ENF} are the sums of three contributions: the first addend depends on the sublaminates' bending stiffness, according to Euler-Bernoulli beam theory; the second addend is due to transverse shear deformability, in line with Timoshenko's beam theory; lastly, the third addend is due to the deformability of the elastic interface. Furthermore, both C_{DCB} and C_{ENF} are expressed by cubic polynomials of the delamination length, a , except for an exponential term (negligible in most cases) appearing in the expressions for C_{ENF} . Thus, the EBT model provides a rationale for some semi-empirical relationships of the literature (Martin and Hansen 1997). Lastly, for what follows, it is important to note that C_{DCB} depends on k_z (through λ_1 and λ_2) and not on k_x and, conversely, C_{ENF} depends on k_x (through λ_3) and not on k_z .

2.3. Energy release rate

Under I/II mixed-mode fracture conditions, the energy release rate can be written as $G = G_I + G_{II}$, where G_I and G_{II} are the contributions related to fracture modes I and II, respectively (Adams et al. 2003). For the MMB test specimen,

$$G_I = \frac{P_I^2}{2B} \frac{dC_{DCB}}{da} \quad \text{and} \quad G_{II} = \frac{P_{II}^2}{2B} \frac{dC_{ENF}}{da}, \quad (4)$$

where

$$P_I = \frac{1}{2} \left(\frac{c+d}{L} + \frac{c}{d} - 1 \right) P \quad \text{and} \quad P_{II} = \left(1 + \frac{c}{d} \right) P \quad (5)$$

are the loads responsible for fracture modes I and II, respectively. By substituting Eqs. (2) into (4), we obtain

$$G_I = \frac{P_I^2}{B^2 D_1} (a + \chi_I h)^2 \quad \text{and} \quad G_{II} = \frac{P_{II}^2}{16 B^2 D_1} \frac{A_1 h^2}{A_1 h^2 + 4 D_1} (a + \chi_{II} h)^2, \quad (6)$$

where

$$\chi_I = \frac{1}{h} \left(\frac{1}{\lambda_1} + \frac{1}{\lambda_2} \right) = \frac{1}{h} \sqrt{\frac{D_1}{C_1}} + \sqrt{\frac{2D_1}{k_z}} \quad \text{and} \quad \chi_{II} = \frac{1}{h} \frac{1}{\lambda_5} = \frac{1}{h} \frac{1}{\sqrt{2k_x \left(\frac{1}{A_1} + \frac{h^2}{4D_1} \right)}} \quad (7)$$

are crack length correction parameters, analogous to those defined for unidirectional specimens (ASTM 2006).

3. Compliance calibration strategy

The values of the elastic interface constants can be obtained through a nonlinear least squares fitting procedure. To this aim, DCB and ENF tests are conducted on specimens obtained from the laminate under examination. As a result, we obtain the experimental measures of the mode I compliance, $C_{DCB,i}$, for a set of delamination lengths, a_i (with $i = 1, 2, \dots, n$), and mode II compliance, $C_{ENF,j}$, for a set of delamination lengths, a_j (with $j = 1, 2, \dots, m$). The sums of the squares of the residuals of the two sets of experimental data are

$$R_I^2 = \sum_{i=1}^n [C_{DCB,i} - C_{DCB}(k_z)]^2 \quad \text{and} \quad R_{II}^2 = \sum_{j=1}^m [C_{ENF,j} - C_{ENF}(k_x)]^2. \quad (8)$$

In order to minimise the above sums, the following necessary conditions are imposed

$$\frac{d}{dk_z} (R_I^2) = -2 \sum_{i=1}^n [C_{DCB,i} - C_{DCB}(k_z)] \frac{dC_{DCB}}{dk_z} = 0 \quad \text{and} \quad \frac{d}{dk_x} (R_{II}^2) = -2 \sum_{j=1}^m [C_{ENF,j} - C_{ENF}(k_x)] \frac{dC_{ENF}}{dk_x} = 0. \quad (9)$$

The derivatives of C_{DCB} and C_{ENF} can be calculated analytically from Eqs. (2) and (3), albeit their expressions are omitted here for the sake of brevity. The numerical solution of Eqs. (9) furnishes the calibrated values of k_z and k_x .

4. Experimental tests

Experimental tests have been conducted on a set of unidirectional laminated specimens obtained from a typical carbon fibre/epoxy matrix composite laminate. Average material properties are the following: longitudinal Young’s modulus $E_x = 116$ GPa, transverse shear modulus $G_{zx} = 0.5$ GPa. Average dimensions of the specimens’ cross sections are $B = 25.3$ mm, $H = 2.8$ mm.

First, DCB tests have been conducted on 250 mm long specimens (Fig. 2a), until a total delamination length of about 100 mm had been achieved (AECMA 1995a). Next, ENF tests have been conducted on the same specimens (Fig. 2b), after a residual part of the delaminated portion had been cut off (AECMA 1995b).

Figures 3a and 3b show the typical load–displacement plots obtained from the DCB and ENF tests, respectively. The ENF tests have been conducted within the elastic range of behaviour at several values of the delamination length in order to measure the compliance. For $a = 20$ mm, the ENF tests have been continued until the onset and growth of the delamination to determine the critical energy release rate.

Table 1 shows the values of the elastic interface constants obtained for the tested specimens via the compliance calibration strategy. In addition, the table lists the values of critical energy release rate deduced through Eqs. (6).

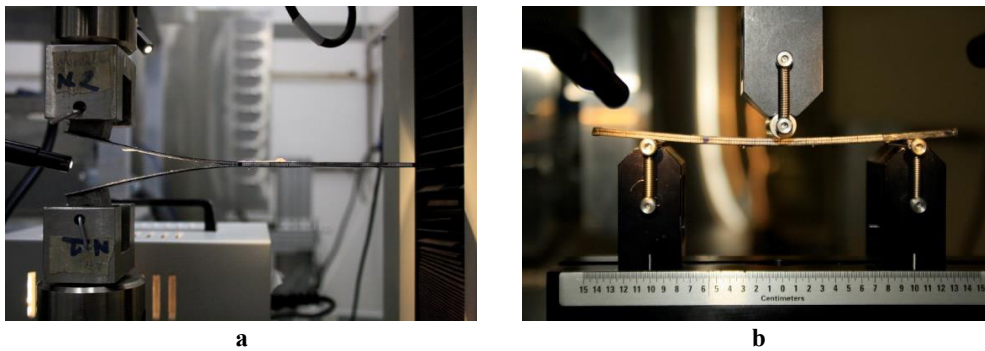


Fig. 2. Experimental tests: (a) DCB test; (b) ENF test.

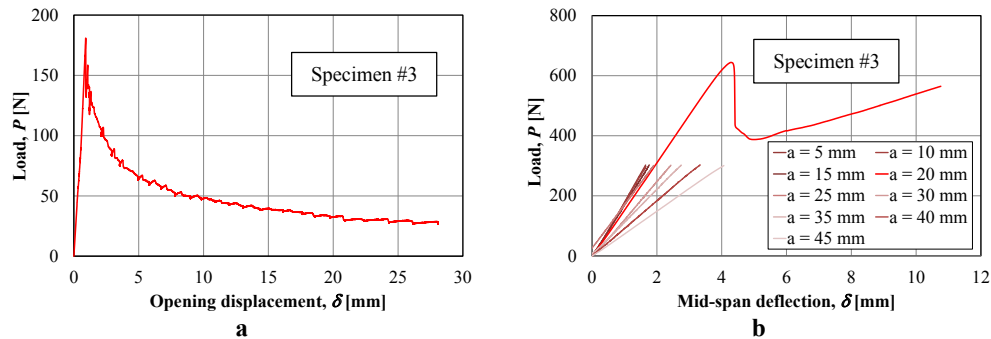


Fig. 3. Load–displacement plots: (a) DCB test; (b) ENF test.

Table 1. Elastic interface constants and critical energy release rates.

Specimen No.	k_z (N/mm ³)	k_x (N/mm ³)	G_{Ic} (J/m ²)	G_{IIc} (J/m ²)
1	41.0	104.6	335.8	1295.6
2	112.7	203.7	603.6	1271.1
3	101.8	634.5	471.6	841.5
Average	85.2	314.3	470.3	1136.1

Figures 4a and 4b show the typical plots of compliance vs. delamination length obtained for the DCB and ENF tests, respectively. Black circles represent the experimental data. Dashed blue lines are the predictions of the simple beam-theory (SBT) model, which is known to underestimate the actual specimen's compliance (Adams et al. 2003). Continuous red lines are the predictions of the EBT model based on the calibrated values of the elastic interface constants. For larger delamination lengths, we note some discrepancies between the EBT model's predictions and experimental data. Such discrepancies may be due to the geometric nonlinearities occurring at higher load levels.

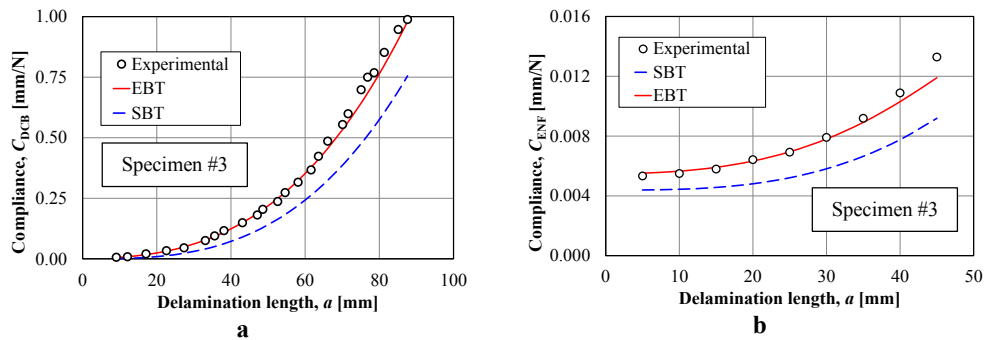


Fig. 4. Compliance vs. delamination length: (a) DCB test; (b) ENF test.

5. Conclusions

We have illustrated an experimental compliance calibration strategy, which enables the estimation of the elastic interface constants used in the enhanced beam-theory model of the MMB test. DCB and ENF tests have been conducted and the interface parameters have been obtained through a nonlinear least squares fitting procedure. MMB tests are currently in progress; their results will be the subject of future publications.

Acknowledgements

The authors wish to thank Alessandra Passaro and Antonella Tarzia of the CETMA consortium (Brindisi, Italy) for their valuable support in conducting the experimental tests.

The financial support of the Italian Ministry of Education, University and Research (MIUR) under programme PRIN 2008 "Light structures based on multiscale material in civil engineering: stiffness and strength, assembly and industrial repeatability" (Prot. N. 20089RJKN_002) is gratefully acknowledged.

References

- Adams, D.F., Carlsson, L.A., Pipes, R.B., 2003. *Experimental Characterization of Advanced Composite Materials*, 3rd edition. CRC Press, Boca Raton.
- AECMA, 1995a. prEN 6033:1995 – Determination of interlaminar fracture toughness energy. Mode I – G_{Ic} . European Association of Aerospace Industries, Bruxelles.
- AECMA, 1995b. prEN 6034:1995 – Determination of interlaminar fracture toughness energy. Mode II – G_{IIc} . European Association of Aerospace Industries, Bruxelles.
- ASTM, 2006. D6671/D6671M-06 – Standard Test Method for Mixed Mode I-Mode II Interlaminar Fracture Toughness of Unidirectional Fiber Reinforced Polymer Matrix Composites. American Society for Testing and Materials, West Conshohocken.
- Bennati, S., Fiscaro, P., Valvo, P.S., 2013a. An enhanced beam-theory model of the mixed-mode bending (MMB) test – Part I: literature review and mechanical model. *Meccanica* 48, 443–462.
- Bennati, S., Fiscaro, P., Valvo, P.S., 2013b. An enhanced beam-theory model of the mixed-mode bending (MMB) test – Part II: applications and results. *Meccanica* 48, 465–484.
- Jones, R.M., 1999. *Mechanics of composite materials*, 2nd edition. Taylor & Francis Inc., Philadelphia.
- Martin, R.H., Hansen, P.L., 1997. Experimental compliance calibration for the mixed-mode bending (MMB) specimen. In: Armanios, E.A. (Ed.), *Composite Materials: Fatigue and Fracture (Sixth Volume)*, ASTM STP 1285, pp. 305–323.